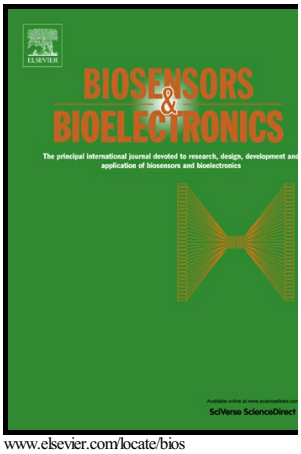

Ultrasensitive electrochemical immunosensor based on horseradish peroxidase (HRP)-loaded silica-poly(acrylic acid) brushes for protein biomarker detection

Yan Zhao, Yiqun Zheng, Rongmei Kong, Lian Xia, Fengli Qu

www.elsevier.com/locate/bios

PII: S0956-5663(15)30392-4
DOI: http://dx.doi.org/10.1016/j.bios.2015.08.065
Reference: BIOS7961

To appear in: *Biosensors and Bioelectronic*

Received date: 1 July 2015
Revised date: 17 August 2015
Accepted date: 28 August 2015

Cite this article as: Yan Zhao, Yiqun Zheng, Rongmei Kong, Lian Xia and Fengl Qu, Ultrasensitive electrochemical immunosensor based on horseradis peroxidase (HRP)-loaded silica-poly(acrylic acid) brushes for protein biomarke detection, *Biosensors and Bioelectronic* http://dx.doi.org/10.1016/j.bios.2015.08.065

Ultrasensitive electrochemical immunosensor based on horseradish peroxidase (HRP)-loaded silica-poly(acrylic acid) brushes for protein biomarker detection

Yan Zhao,[†] Yiqun Zheng,[‡] Rongmei Kong,[†] Lian Xia,[†] and Fengli Qu[†,*]

[†] The Key Laboratory of Life-Organic Analysis, College of Chemistry and Chemical Engineering, Qufu Normal University, Qufu, Shandong 273165, P. R. China

[‡] Leadernano Tech. L.L.C., Jining, Shandong 272000, P. R. China

[*] Corresponding author: Prof. F. Qu, Tel/fax: (+86) 537-4456301
E-mail: fengliquhn@hotmail.com

Abstract

We report an ultrasensitive electrochemical immunosensor designed for the detection of protein biomarkers using horseradish peroxidase (HRP)-loaded silica-poly(acrylic acid) brushes (SiO_2-SPAABs) as labels. HRP could be efficiently and stably accommodated in the three-dimensional architecture of the SiO_2-SPAABs and the SiO_2-SPAABs-HRP exhibited high catalytic performance towards o-phenylenediamine (OPD) oxidation in the presence of H_2O_2, which resulted in significant differential pulse voltammetric (DPV) response change and color change. Using human IgG (HIgG) as a model analyte, a sandwich-type immunosensor was constructed. In particular, graphene oxide (GO) and SiO_2-SPAABs-HRP were used to immobilize capture antibody (Ab_1) and bind a layer of detection antibody (Ab_2), respectively. The current biosensor exhibited a good linear response of HIgG from 100 pg/mL to 100 μg/mL with a detection limit of 50 pg/mL (S/N = 5). The sensitivity

was 6.70-fold higher than the conventional enzyme-linked immunosorbent assays. The immunosensor results were validated through the detection of HIgG in serum samples.

Key words: Enzyme catalysis; electrochemical immunoassay; protein biomarker; silica-poly(acrylic acid) brushes; horseradish peroxidase

Introduction

During the past decades, the detection of protein biomarkers has been of great importance to the diagnosis and treatment of proteomics diseases (Addona et al. 2011), and the detection of drug discovery (Schirle et al. 2012), infectious agents (Giri et al. 2011), and warning against bio-warfare agents (Haynes et al. 2005). Due to the advantages in specificity and stability, various immunoassays based on hybridization or antibody-antigen interaction have been reported, including fluorescence immunoassay (Li et al. 2014), surface plasmon resonance (SPR) immunoassay (Yu et al. 2013), quartz crystal microbalance (QCM) immunoassay (Akter et al. 2015), and electrochemistry immunoassay (Chikkaveeraiah et al. 2012; Raj kumar et al. 2015; Ranjani et al. 2015). Among these options, the electrochemical technique becomes attractive for the immunoassay of protein biomarkers, owing to its high sensitivity, inherent simplicity, miniaturization, and low cost. For typical electrochemical immunoassays, detection probes are usually included to monitor the signal change as induced by protein biomarkers. The ultrasensitive detection of protein biomarkers often requires signal amplification strategies on immunosensor tags. For different kinds of signal amplification methods, many electrochemical tags have been studied and developed, including enzymes (Hou et al. 2014; Lai et al. 2011), metal ions (Ranjani et al. 2015; Salamon et al. 2015; Wang 2012), electron mediator (Gnana kumar et al. 2014; Li et al. 2011; Senthilkumar et al. 2014) and quantum dots (Lin et al. 2011).

Compared to other counterparts, enzymes, such as horseradish peroxidase (HRP), possess remarkable advantages such as high substrate specificities and high efficiency

under mild conditions (Martin and Ames 1961). To this end, HRP-loaded immunosensors have been widely used for laboratorial and clinical analysis owing to their simplicity, low cost, easy operation and instrumentation (Su et al. 2012). However, conventional HRP-antibody conjugated immunoassay has been plagued with low-abundant capacity (Yang et al. 2010). Worse still, HRP can be easily denatured by environment changes since their catalytic activity depends on their integrity protein conformation (Liu et al. 2013). So it has become quite essential to enhance the stability and persistence of HRP-loaded immunoassays.

Currently, the most typical way to prepare HRP-loaded labels is covalent immobilization of enzyme on nanoparticles via well-established conjugation methods (Deng et al. 2012; Merola et al. 2014). In particular, nanoparticles, composed of gold (He et al. 2013), polymers (Darain et al. 2003), magnetite (Weizmann et al. 2003), silica (SiO_2) (Qian et al. 2010), or mesoporous silica (Wang et al. 2013), etc., are often chosen as a supporting matrix to increase the loading amount of HRP to enhance the detection sensitivity. However, these materials are plagued with the problems of a relatively low enzyme loading capacity and a significant loss of enzyme activity during the immobilized process, which limited their further applications and uses. For instance, HRP could only be immobilized on the surface of mesoporous silica nanoparticles due to the space steric hindrance. The larger specific surface area could not guarantee the capacity and activity of enzymes (Chen et al. 2011; Shen et al. 2015).

Herein, we describe a facile method to enhance the stability and persistence of HRP-loaded immunoassays. The success of this work relies on the use of poly(acrylic acid) brushes (SPAABs) to modify the surface of SiO_2 nanoparticles and the resultant SiO_2-SPAABs serves as an ideal scaffold for stable and large-quantity enzyme loading with good biological activities. In this structure, the SiO_2 nanoparticles serve as a robust and versatile core for surface modification (Ghosh Chaudhuri and Paria 2011; Guerrero‐Martínez et al. 2010) and surface-initiated reversible addition-fragmentation chain transfer (RAFT) polymerization process of SPAABs provided a good control of molecular weights, rich content of carboxyl groups and

thickness of the poly(acrylic acid) (PAA) brushes (Qu et al. 2013). As a result, SiO_2-SPAABs nanoparticles exhibit many superior properties over conventional nanoparticles: the three-dimensional structure, flexibility and high-abundant capacity of enzyme.

After HRP was loaded on SiO_2-SPAABs, an ultrasensitive electrochemical immunosensor was designed for the detection of protein biomarkers. HIgG was used as a model detection target to develop a SiO_2-SPAABs-HRP-based electrochemical immunoassay. SiO_2-SPAABs-HRP was employed as a catalytically label to bind a layer of immosensing antibody (Ab_2) and GO was used as a capture probe to immobilize capture antibody (Ab_1). The sandwich-type immunocomplex had insignificant DPV signal, while it could catalyze the oxidation of o-phenylenediamine (OPD), along with a significant color change from colorless to red and a differential pulse voltammetric (DPV) response change at -0.514 V. Due to the presence of high-abundant capacity of HRP in the SiO_2-SPAABs, a signal amplification strategy for ultrasensitive detection of HIgG was successfully developed. In addition, the use of GO could increase the antibody loading and accelerated the electron transfer. The dynamic range of the developed electrochemical immunoassay could reach 100 pg/mL to 100 μg/mL toward HIgG with a detection limit of 50 pg/mL (S/N = 5) and a correlation coefficient of 0.995 with good stability and selectivity.

1 Experimental section

1.1 Reagents and apparatus

Human IgG (HIgG) and anti-human IgG (Ab) were obtained from Shanghai Linc-Bio Science Co. LTD. HRP (250 U/mg), Graphite and H_2O_2 were purchased from Sinopharm Chemical Reagent Co. LTD. (Shanghai, China). N-(3-dimethylaminopropyl)-N′-ethyl-carbodiimidehydrochloride (EDC), N-hydroxysuccinimide (NHS) and o-phenylenediamine (OPD) were purchased from Aladdin Industrial Inc. (Shanghai, China). All chemicals in this study were obtained from the manufactures without purification unless specifically noted. All solutions were prepared with deionized water (resistivity > 18 MΩ•cm) produced using a

Millipore system. Buffer was used for all the assays and dilutions.

Electrochemical measurements were performed on a CHI 760D electrochemical workstation (Shanghai CH Instruments Co., China). A conventional three-electrode system was used for all electrochemical measurements, a glassy carbon electrode (GC, 4 mm in diameter) as the working station, an Ag/AgCl electrode as the reference electrode, and a platinum wire electrode as the counter electrode. Transmission electron microscope (TEM) images were obtained using a JEM-2100 microscope operated at 200 kV. UV/vis measurements were performed using a Varian Cary-300 bio UV/vis spectrophotometer (USA). Thermo gravimetric analysis (TGA) measurements were performed using a Hitachi (DMA7100) TGA at a heating rate of 10 °C/min. Gel permeation chromatography (GPC) results were obtained by using a Polymer-GPC220.

1.2 Preparation of SiO_2-SPAABs

SiO_2-SPAABs were synthesized via surface-initiated reversible addition–fragmentation chain transfer (RAFT) polymerization on SiO_2 NPs (Qu et al. 2013). SiO_2 NPs with a diameter of 40 nm were prepared via the Stöber method (Stöber et al. 1968). Table S1 listed the main parameters for the synthesis of SiO_2-SPAABs.

1.3 Preparation of SiO_2-SPAABs-HRP-Ab_2

SiO_2-SPAABs-HRP was synthesized by covalently immobilizing HRP in SiO_2-SPAABs using the “chemical conjugation after electrostatic entrapment” (CCEE) process (Qu et al. 2014). In particular, 0.03 g of SiO_2-SPAABs were suspended in 5 mL of 2-(N-morpholino) ethanesulfonic acid buffer (10 mmol/L) containing 0.05 wt% Tween-20 (MES buffer, pH = 5.0) and mixed with HRP for 20 min at room temperature. After removing the excessive HRP via centrifugation, 1 mL of EDC (0.5 mmol/L) was added for the electro statically absorption of HRP, and this conjugation process was conducted for 2 h at room temperature. After centrifugation and discarding the supernatant, the SiO_2-SPAABs-HRP was obtained and stored at 4 °C with a concentration of 30 mg/mL (in terms of SiO_2-SPAABs).

The mouse anti-human IgG antibody (Ab_2) was conjugated to the periphery of

the brushes via NHS/EDC process. 1 mL of the as-prepared SiO_2-SPAABs-HRP complex was activated by 0.1 mol/L NHS and EDC for 20 min at room temperature and centrifuged with MES three times to remove excess reagents. Then 50 μL of Ab_2 (5 μg/mL) was added and the conjugation was completed after 2 h at 37 °C. After the conjugation and centrifugation, the obtained SiO_2-$SPAAB_S$-HRP-Ab_2 was blocked by 1 wt% BSA and stored in phosphate buffer saline containing 0.05 wt% Tween-20 (PBS buffer, pH = 7.2) at 4 °C with a final concentration of 3 mg/mL.

1.4 Sandwich-type electrochemical immunosensing

Graphene oxide (GO) was prepared using Hummer's method (McAllister et al. 2007) and used to immobilize the goat anti-Human IgG antibody (Ab_1) for the fabrication of the electrochemical immunosensor. 100 mmol/L of EDC and 100 mmol/L of NHS were added into 1 mL of GO solution (2 mg/mL). After being stirred for 4 h and centrifugation, 50 μL of Ab_1 (5 μg/mL) was added into the mixture. 2 hours later, the GO-Ab_1 was centrifuged and stored in 4 °C before use with a final concentration of 2 mg/mL. 10 μL of GO-Ab_1 buffer solution was dropped onto the GC electrode, the electrode was washed with PBS buffer (pH =7.2) after drying naturally and incubated in 1 wt% BSA solution for 1 h to prevent nonspecific adsorption between the antigen and the electrode surface. Thereafter, various concentrations of HIgG were added onto the electrode and incubated for 0.5 h at 37 °C, respectively. The electrode was washed extensively to remove unbounded HIgG. Subsequently, 10 μL of as-prepared SiO_2-SPAABs-HRP-Ab_2 was dropped onto the electrode and incubated for another 1 h at 37 °C. After rinsed thoroughly with PBS buffer solution, the electrode was ready for measurement. DPV measurements were performed in the PBS buffer solution containing 2.0 mmol/L OPD and 4.0 mmol/L H_2O_2 using a conventional three-electrode system.

2 Results and discussion

2.1 Sensing mechanism and the characterization of the SiO_2-SPAABs-based electrochemical immunosensor

Scheme 1 showed the sensing mechanism of our immunoassay. GO was utilized

to immobilize the capture antibody (Ab_1) covalently, which increased the antibody loading and accelerated the electron transfer. As shown in Scheme 1A, the SiO_2-SPAABs used in this study are monodispersed colloidal particles with a 40-nm SiO_2 core and densely grafted PAA chains formed via surface RAFT polymerization. The PAA brushes, with abundant carboxyl groups, were particularly suitable for the CCEE process. Key structural parameters of SiO_2-SPAABs were listed in Table S1. SiO_2−COOH was used for comparison. In aqueous solution, the SiO_2-SPAABs feature long-stretching PAA chains with high grafting density, abundant carboxyl groups, uniform distribution and excellent monodispersion. SiO_2-SPAABs nanoparticle exhibits many superior properties over conventional nanoparticles, including the three-dimensional construction, flexibility, biocompatibility and high-abundant capacity of enzyme. After the immobilization with HRP, the SiO_2-SPAABs-HRP was decorated with a corona of mouse anti-human IgG antibody (Ab_2) via the NHS/EDC process to obtain SiO_2-SPAABs-HRP-Ab_2. DPV detection was achieved by a sandwich assay using GO-Ab_1 to capture antigen (Scheme 1B). Accompanied with the oxidation of OPD by HRP/H_2O_2, a color change from colorless to redness and a DPV response change at -0.514 V can be observed.

Figure 1 showed TEM images of GO (Fig. 1A), SiO_2 NPs (Fig. 1B), and SiO_2-SPAABs (Fig. 1, C and D). These materials were dispersed in MES buffer (pH = 5). The morphological character of GO exhibited as an ultrathin transparent nanosheet, which was highly beneficial in accelerating the electron transfer. The SiO_2 NPs were quasi-spherical with an average diameter of around 40 nm. Figure 1, C and D exhibited core-shell structure of SiO_2-SPAABs. It clearly showed that the SiO_2 core was capped by the spherical PAA brushes with an average thickness of 20 nm.

Successful immobilization of HRP on SiO_2-SPAABs could be visually observed (Fig. 2A). To validate the contribution of the unique structure of SiO_2-SPAABs-HRP, conventional carboxylated SiO_2 nanoparticles (SiO_2−COOH) with the size of 40 nm were also prepared and conjugated with HRP via the NHS/EDC process at optimized conditions. After the immobilization, SiO_2-SPAABs-HRP exhibited a characteristic brownish color of HRP while the SiO_2−COOH-HRP showed a more light brownish

color. This is because free HRP could not be separated by centrifugation while immobilized HRP (SiO_2-SPAABs-HRP and SiO_2−COOH-HRP) could be separated by centrifugation, leaving the supernatant colorless. The color change of nanoparticles and their response to centrifugation indicated the success of HRP immobilization. As shown in Figure 2B, SiO_2-SPAABs-HRP complex was measured using UV/vis spectrometry, the characteristic absorbance of HRP was clearly observed in SiO_2-SPAABs-HRP, demonstrating its successful immobilization on SiO_2-SPAABs. With the same concentration, the characteristic absorbance of SiO_2-HRP was weaker than that of SiO_2-SPAABs-HRP, indicating that more HRP was immobilized on SiO_2-SPAABs.

The enzyme binding capacity was also estimated to be about 397 μg/mL by subtracting the background absorption of SiO_2-SPAABs (which was fitted by an exponential function (Duan et al. 2014)) and comparing with the absorbance peak intensity of free HRP located at 403 nm. Furthermore, no leaking of HRP was observed after SiO_2-SPAABs-HRP was re-dispersed in PBS for weeks without noticeable precipitation. The binding capacity of SiO_2−COOH was estimated to be 8.2 μg/mL by the depletion method, much less than achieved using SiO_2-SPAABs.

Electrochemical impedance spectroscopy (EIS) is an effective method for monitoring the electrode assembly process. Different modified electrodes were conducted in 0.1 mol/L KNO_3 containing 5 mmol/L $K_3[Fe(CN)_6]$/ $K_4[Fe(CN)_6]$ solution with frequency varied from 100 kHz to 0.1 Hz at a potential of 0.241 V. As shown in Figure S2, a semicircle at higher frequencies and a linear curve at lower frequencies were obtained at each electrode. After the modification of the electrode with GO-Ab_1, the electrode showed a higher resistance (curve b) than the bare GC (curve a). When the electrode was incubated in BSA solution and HIgG buffer solution, the resistance further increased (curve c and curve d). Subsequently, after the capture of SiO_2-SPAABs-HRP-Ab_2, the resistance increased again (curve e). The main reason could be attributed to the insulating ability of proteins. These results proved that the electrode was fabricated as expected.

2.2 Optimization of the immunoassay conditions

The electrochemical catalytic property of SiO_2-SPAABs-HRP was measured using OPD/H_2O_2 as the substrate. An appropriate concentration of OPD and H_2O_2 was necessary for the optimal response. As shown in Figure S3A, increasing the concentration of OPD and H_2O_2 in the solution could increase the signal for the sandwich immunosensor. Therefore, 2.0 mmol/L OPD and 4.0 mmol/L H_2O_2 were selected for the detection.

The concentration of SiO_2-SPAABs was another important factor for the signal response. The effect of the concentration of SiO_2-SPAABs on the DPV response was investigated (Figure S3B). At room temperature, under the detection 10 μg/mL of HIgG, the DPV response increased with the increasing concentration of SiO_2-SPAABs and then stabilized, which indicated the achievement of saturated binding in the immunoreactions. Thus, 3.0 mg/mL SiO_2-SPAABs was chosen for the following experiments.

Temperature and incubation time could also influence the detection sensitivity of the developed immunoassay. Considering the practical application of the proposed system in clinical testing, the incubation temperature was set at 37 °C. The effect of incubation time was investigated with the detection of 10 μg/mL of HIgG. The DPV response intensity increased with the increased incubation time and tended to level off after 60 min (Fig. S3C). Therefore, incubation time of 60 min was used for the detection of HIgG in this study.

2.3 Analytical performance of the immunosensor

The analytical performance of this immunosensor was evaluated by applying 10 μL of various concentrations of HIgG under the above-mentioned optimized conditions. The DPV signal intensity increased as HIgG concentration increased (Fig. 3). The DPV responses and the corresponding calibration curves were shown in Figure 4A (line a). As concentration of HIgG increased, good correlation between the HIgG concentration logarithm and the DPV response was observed with a wide dynamic range (from 100 pg/mL to 100 μg/mL), which corresponded to the levels that occur naturally in human blood plasma or serum. The linear regression equation was $I_{SiO2\text{-}SPAABs\text{-}HRP} = 50.87 + 4.53 \lg (C_{HIgG})$ ($R^2 = 0.994$), where I (μA) was the DPV

response and C (g/mL) was the concentration of the protein biomarker. The limit of detectable concentration was 50 pg/mL at S/N = 5.

2.4 Estimation of signal amplification function

As shown in Figure S4, the SiO_2-SPAABs-HRP-based nanobioprobes detected on the electrode surface led to a much higher response (curve a) than the nonspecific adsorption of the nanobioprobes without antigen (curve d). To verify the SiO_2-SPAABs-HRP-assisted signal amplification, SiO_2-HRP labeled antibody and HRP directly labeled antibody were used to complete the sandwich immunoreactions (curve c and curve d), and comparatively lower responses were obtained, which indicated that the presence of SiO_2-SPAABs-HRP efficiently enhanced the overall signal detected. As indicated in Figure 4A (line b and line c), both controlled systems exhibited excellent linearity for the analyte concentration ranges tested. The linear regression equation is $I_{SiO2\text{-}HRP} = 22.23 + 1.77 \lg (C_{HIgG})$ ($R^2 = 0.995$), $I_{HRP} = 13.95 + 0.97 \lg (C_{HIgG})$ ($R^2 = 0.990$), respectively. By comparing the slope values of these linear curves, the DPV response of SiO_2-SPAABs based label exhibited a response rate nearly 2.56-fold higher than SiO_2 nanoparticle labels and 6.70-fold higher than HRP labeled antibodies, the dramatic amplification of signal was intuitive visually in Figure 4B, which indicated that the presence of SiO_2-SPAABs based labels efficiently accelerated the electron transfer and further enhanced the overall signal detected.

The high sensitivity indicated the success of this signal amplification strategy for the detection of HIgG. Moreover, these facile synthesized SiO_2-SPAABs-based labels and time-saving electrochemical method exhibited a wide linear dynamic range than those for HIgG detection documented in literatures (Tab. S2). Due to the designed signal amplification, the proposed immunoassay not only avoided the spilling of enzyme substrate in the detected electrode and exhibited high enzyme activities for a long time, but also proposed an appropriate detection range with a low detection limit.

2.5 Specificity, reproducibility, and stability

Good specificity for target analysis is necessary for a new designed sensing system with potential applications for real samples. To evaluate the specificity of the developed signal amplified immunoassay for HIgG, several potential interfering

compounds were investigated under the same conditions. The 10 μg/mL of HIgG containing 100 μg/mL interference substances were measured by the immunoassay. As shown in Figure 5, only HIgG caused a dramatic DPV signal increase. Glucose, Human serum albumin (HSA), prostate-specific antigen (PSA), and carbohydrate antigen 125 (CA125) triggered negligible signal change. The inset graph showed this result intuitively, indicating that the selectivity of the immunoassay was quite acceptable and the common component existed in the human serum did not interfere the detection of HIgG.

To evaluate the reproducibility of the immunosensor, three working electrodes were prepared for the detection of 10 μg/mL HIgG. The relative standard deviation (RSD) of the measurement for the three electrodes was 1.9%, suggesting the precision and reproducibility of the proposed immunosensor was quite good.

The stability of the immunoassay is also a key factor in the practical application. In this work, the stability of the immunoassay was tested using 10 μg/mL of HIgG as a model analyte. The DPV response of the immunoassay decreased only 2.4% after 7 days and 8.5% after 1 month storage in a refrigerator at 4 °C in a PBS buffer solution.

2.6 Analysis of complex biological samples

To evaluate the clinical application potential of the proposed immunosensor, a recovery test of HIgG in human serum was performed. Three diluted human serum samples (1%) were performed for the detection of HIgG using standard addition method. The recovery percentage of HIgG detected by the immunosensor in serum samples ranged from 92.89% to 105.37%, and the RSD was ranged from 0.49% to 8.61%, which were satisfactory for quantitative assays performed in biological samples (Tab. S3).

3 Conclusion

In summary, the SiO_2-SPAABs-HRP-based ultrasensitive enzymatic immunosensor for protein biomarkers detection has been successfully developed. The high capacity and high activity for covalent immobilization of HRP in SiO_2-SPAABs endowed SiO_2-SPAABs-HRP with remarkable signal amplification capability. Using

HIgG as a model analyte, the immunosensor was simply prepared based on a sandwich-type protocol with the primary antibody immobilized onto the surface of GO. After the fabrication of the immunosensor, the electrode was dipped into the buffer solution containing OPD and H_2O_2. In the presence of HRP, the catalytic oxidation provided DPV response change. The dynamic range of the developed amplified immunoassay for HIgG could achieve 100 pg/mL to 100 μg/mL with a detection limit of 50 pg/mL (S/N = 5). This method was also applied for the analysis of clinical serum samples with satisfactory results, which confirmed its promising practical application.

Acknowledgement

This work was supported by the National Natural Science Foundation of China (21375076, 21205068), the International Science and Technology Cooperation Program of China (2015DFA50060), the Project of Shandong Province Science and Technology Program (2013GGX10207, 2015GSF121031), the Excellent Middle-age and Young Scientists Research Award Foundation of Shandong Province (BS2013SW012), the Natural Science Foundation of Shandong Province (ZR2014BM029) and the Project of University-industry Cooperation of Jining City (2014018).

References

Addona, T.A., Shi, X., Keshishian, H., Mani, D., Burgess, M., Gillette, M.A., Clauser, K.R., Shen, D., Lewis, G.D., Farrell, L.A., 2011. Nat. Biotechnol. 29, 635-643.

Akter, R., Rhee, C.K., Rahman, M.A., 2015. Biosens. Bioelectron. 66, 539-546.

Chen, L., Zhang, Z., Zhang, P., Zhang, X., Fu, A., 2011. Sensors and Actuators B: Chemical. 155, 557-561.

Chikkaveeraiah, B.V., Bhirde, A.A., Morgan, N.Y., Eden, H.S., Chen, X., 2012. ACS nano. 6, 6546-6561.

Darain, F., Park, S.-U., Shim, Y.-B., 2003. Biosens. Bioelectron. 18, 773-780.

Deng, S., Lei, J., Huang, Y., Yao, X., Ding, L., Ju, H., 2012. Chem. Commun. 48, 9159-9161.

Duan, Z., Qu, Z., Hu, F., Yang, Y., Chen, G., Xu, H., 2014. Appl. Surf. Sci. 300, 104-110.

Ghosh Chaudhuri, R., Paria, S., 2011. Chem. Rev. 112, 2373-2433.

Giri, S., Sykes, E.A., Jennings, T.L., Chan, W.C., 2011. ACS nano. 5, 1580-1587.

Gnana kumar, G., Justice Babu, K., Nahm, K.S., Hwang, Y.J., 2014. RSC Advances. 4, 7944-7951.

Guerrero‐Martínez, A., Pérez‐Juste, J., Liz‐Marzán, L.M., 2010. Adv. Mater. 22, 1182-1195.
Haynes, C.L., Yonzon, C.R., Zhang, X., Van Duyne, R.P., 2005. J. Raman Spectrosc. 36, 471-484.
He, J.-L., Tian, Y.-F., Cao, Z., Zou, W., Sun, X., 2013. Sensors and Actuators B: Chemical. 181, 835-841.
Hou, L., Tang, Y., Xu, M., Gao, Z., Tang, D., 2014. Anal. Chem. 86, 8352-8358.
Lai, G., Yan, F., Wu, J., Leng, C., Ju, H., 2011. Anal. Chem. 83, 2726-2732.
Li, H., Wei, Q., He, J., Li, T., Zhao, Y., Cai, Y., Du, B., Qian, Z., Yang, M., 2011. Biosens. Bioelectron. 26, 3590-3595.
Li, Y., Hong, M., Qiu, B., Lin, Z., Chen, Y., Cai, Z., Chen, G., 2014. Biosens. Bioelectron. 54, 358-364.
Lin, D., Wu, J., Yan, F., Deng, S., Ju, H., 2011. Anal. Chem. 83, 5214-5221.
Liu, X., Liu, Y., Zhang, Z., Huang, F., Tao, Q., Ma, R., An, Y., Shi, L., 2013. Chem.-Eur. J. 19, 7437-7442.
Martin, R.G., Ames, B.N., 1961. J. Biol. Chem. 236, 1372-1379.
McAllister, M.J., Li, J.-L., Adamson, D.H., Schniepp, H.C., Abdala, A.A., Liu, J., Herrera-Alonso, M., Milius, D.L., Car, R., Prud'homme, R.K., Aksay, I.A., 2007. Chem. Mater. 19, 4396-4404.
Merola, G., Martini, E., Tomassetti, M., Campanella, L., 2014. Sensors and Actuators B: Chemical. 199, 301-313.
Qian, J., Zhang, C., Cao, X., Liu, S., 2010. Anal. Chem. 82, 6422-6429.
Qu, Z., Chen, K., Gu, H., Xu, H., 2014. Bioconjugate Chem. 25, 370-378.
Qu, Z., Hu, F., Chen, K., Duan, Z., Gu, H., Xu, H., 2013. J. Colloid Interface Sci. 398, 82-87.
Raj kumar, T., Babu, K.J., Yoo, D.J., Kim, A.R., Gnana kumar, G., 2015. RSC Advances. 5, 41457-41467.
Ranjani, M., Sathishkumar, Y., Lee, Y.S., Jin Yoo, D., Kim, A.R., Gnana kumar, G., 2015. RSC Advances. 5, 57804-57814.
Salamon, J., Sathishkumar, Y., Ramachandran, K., Lee, Y.S., Yoo, D.J., Kim, A.R., Gnana kumar, G., 2015. Biosens. Bioelectron. 64, 269-276.
Schirle, M., Bantscheff, M., Kuster, B., 2012. Chem. Biol. 19, 72-84.
Senthilkumar, N., Babu, K.J., Gnana kumar, G., Kim, A.R., Yoo, D.J., 2014. Ind. Eng. Chem. Res. 53, 10347-10357.
Shen, Y., Zhang, Y., Zhang, X., Zhou, X., Teng, X., Yan, M., Bi, H., 2015. Nanoscale. 7, 2941-2950.
Stöber, W., Fink, A., Bohn, E., 1968. J. Colloid Interface Sci. 26, 62-69.
Su, H., Yuan, R., Chai, Y., Zhuo, Y., 2012. Biosens. Bioelectron. 33, 288-292.
Wang, H., Zhang, Y., Yu, H., Wu, D., Ma, H., Li, H., Du, B., Wei, Q., 2013. Anal. Biochem. 434, 123-127.
Wang, J., 2012. Microchimica Acta. 177, 245-270.
Weizmann, Y., Patolsky, F., Katz, E., Willner, I., 2003. J. Am. Chem. Soc. 125, 3452-3454.
Yang, M., Li, H., Javadi, A., Gong, S., 2010. Biomaterials. 31, 3281-3286.
Yu, Q., Zhan, X., Liu, K., Lv, H., Duan, Y., 2013. Anal. Chem. 85, 4578-4585.

Figure Captions

Scheme 1. Schematic illustration of the electrochemical immunoassay protocol: (A) Covalent immobilization of HRP into SiO_2-SPAABs by CCEE process and conjugation of antibody onto

SiO_2-SPAABs-HRP via NHS/EDC process (B) SiO_2-SPAABs amplified sandwich-type immunosensing strategy and signal amplification method.

Figure 1. TEM images of (A) GO (B) SiO_2 NPs and (C, D) SiO_2-SPAABs.

Figure 2. (A) Pictures of aqueous suspensions of SiO_2-SPAABs and SiO_2−COOH before and after immobilizing with HRP. (B) UV/vis spectra of aqueous suspensions of free HRP, SiO_2-SPAABs-HRP, SiO_2-HRP and SiO_2-SPAABs.

Figure 3. The DPV response of OPD oxidation toward different concentration of HIgG.

Figure 4. (A) Calibration curves toward different concentrations of HIgG using various elements of (a) SiO_2-SPAABs-HRP, (b) SiO_2-HRP, and (c) free HRP and (B) the corresponding color variations. Error bar = SD (n = 5).

Figure 5. The specificity of the immunoassay. The inset is the corresponding photographs of color change for the specificity.

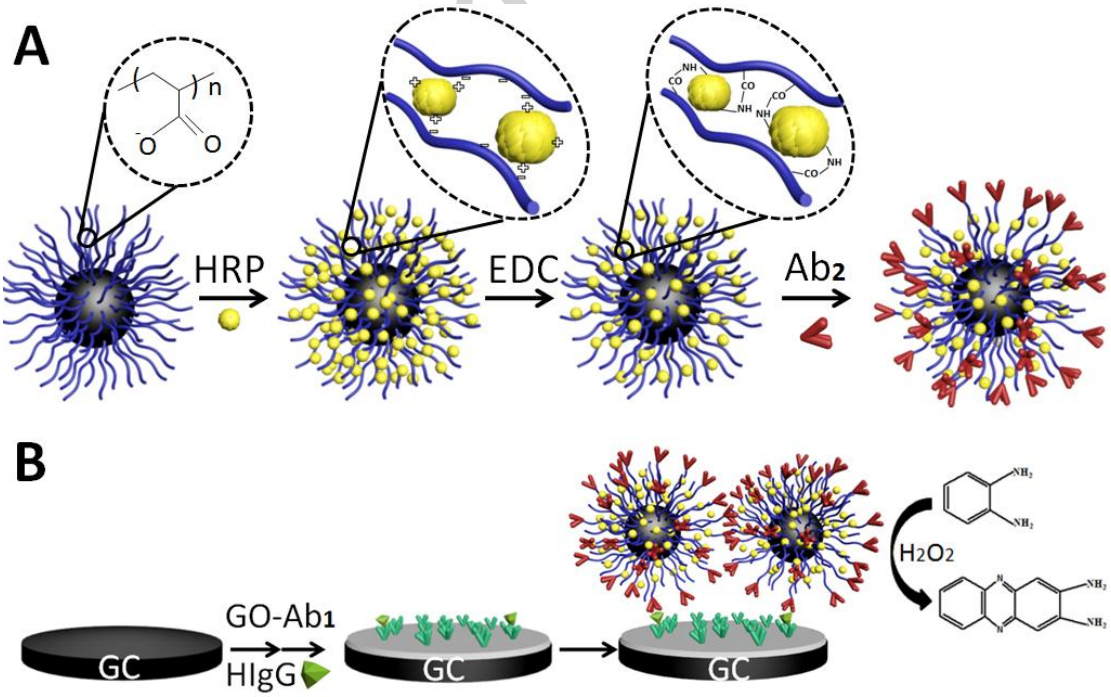

Scheme 1. Schematic illustration of the electrochemical immunoassay protocol: (A) Covalent immobilization of HRP into SiO_2-SPAABs by CCEE process and conjugation of antibody onto SiO_2-SPAABs-HRP via NHS/EDC process (B) SiO_2-SPAABs amplified sandwich-type immunosensing strategy and signal amplification method.

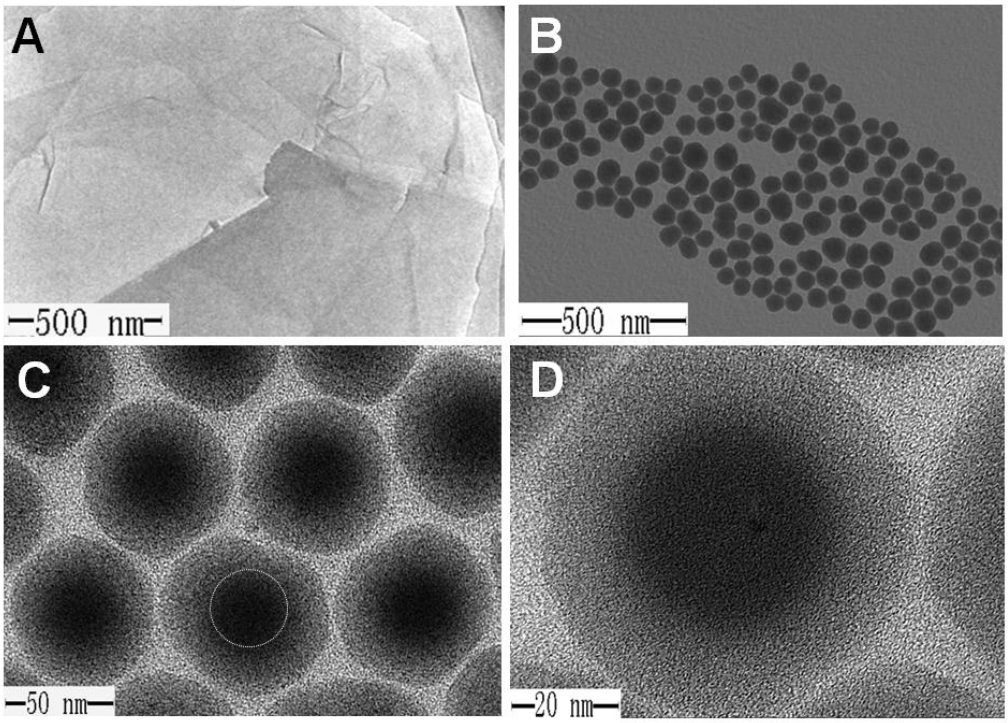

Figure 1. TEM images of (A) GO, (B) SiO_2 NPs and (C, D) SiO_2-SPAABs.

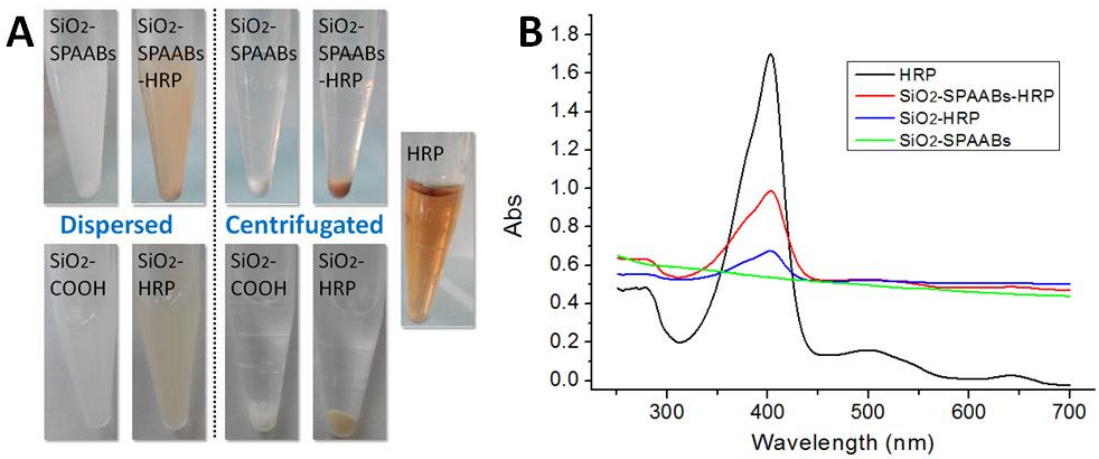

Figure 2. (A) Pictures of aqueous suspensions of SiO_2-SPAABs and SiO_2−COOH before and after immobilizing with HRP. (B) UV/vis spectra of aqueous suspensions of free HRP, SiO_2-SPAABs-HRP, SiO_2-HRP and SiO_2-SPAABs.

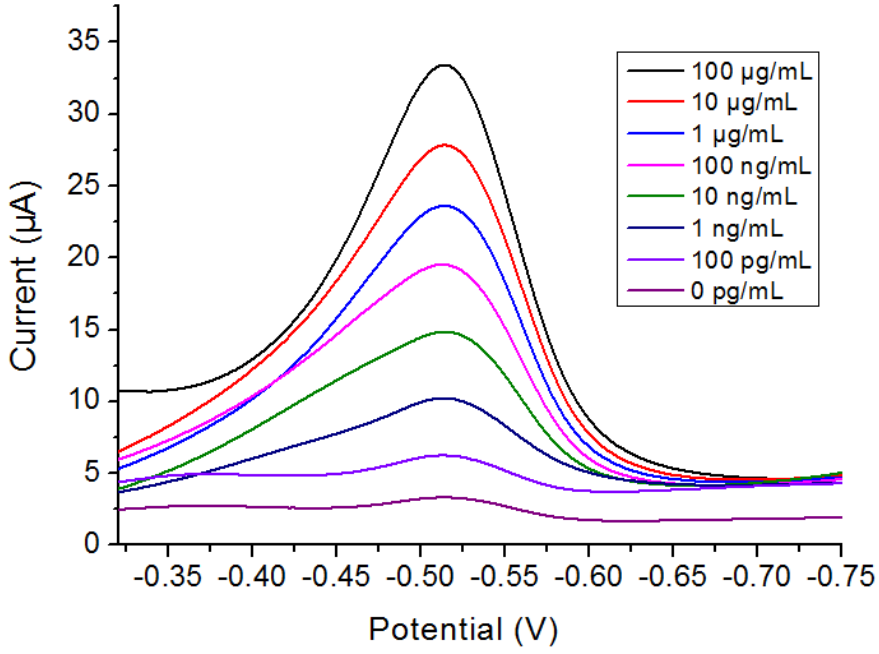

Figure 3. The DPV responses of OPD oxidation toward different concentrations of HIgG.

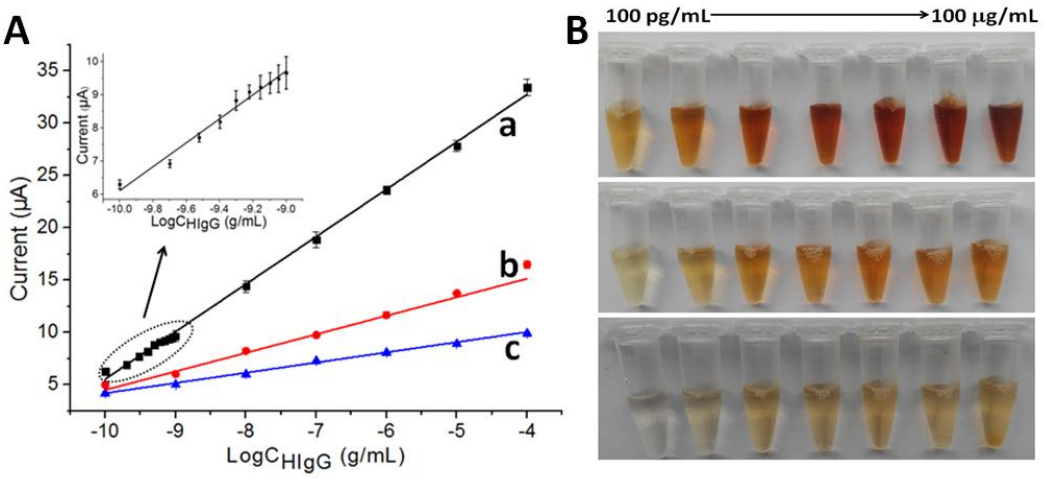

Figure 4. (A) Calibration curves toward different concentrations of HIgG using various elements of (a) SiO_2-SPAABs-HRP, (b) SiO_2-HRP, and (c) free HRP and (B) the corresponding color variations. Error bar = SD (n = 5).

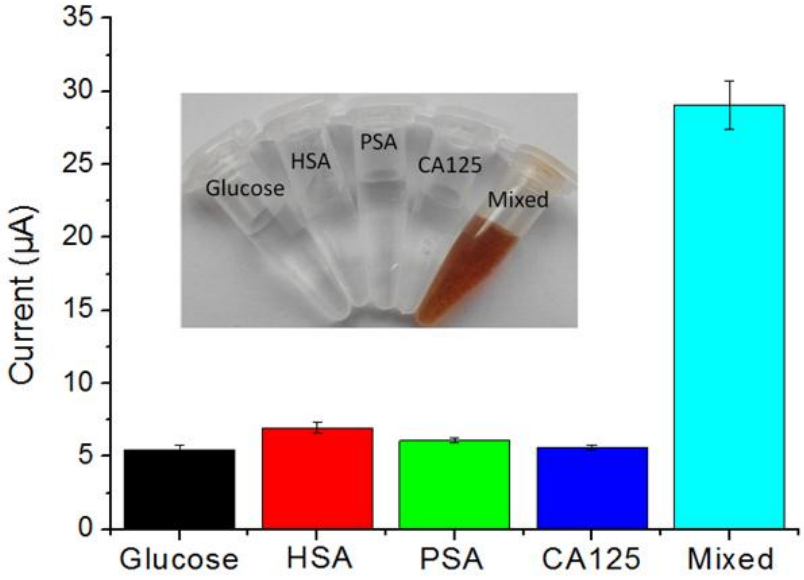

Figure 5. The specificity of the immunoassay. The inset is the corresponding photographs of color

change for the specificity.

Research Highlights

Colorimetric immunoassay was designed for the ultrasensitive detection of HIgG.

Signal amplification was achieved using HRP-loaded SiO_2-SPAABs.

Good performance was obtained with a detection limit of 50 pg/mL.

Favorable results were achieved for detecting HIgG in complex biological samples.